The Laplacian in a stochastic model for spatiotemporal reaction systems

Sebastian Lück Michael Beil Frank Fleischer Stéphanie Portet
Wolfgang Arendt Volker Schmidt

Abstract

We demonstrate how the Laplace operator can be combined with a stochastic jump process to describe the evolution of a polymer network. Growth processes in polymer networks can proceed through the transfer of rather large oligomeric subunits from a pool of soluble molecules into the filaments forming the network. In such a situation stochastic jump processes are a natural tool for the description of network formation at the nanometer scale. However, modeling of the reaction system in high spatiotemporal resolution also needs to capture the evolution of the soluble filament precursor molecules, which controls local properties of the growth process. We illustrate how this may be achieved by combining a deterministic diffusion equation with a stochastic jump process within the setting of a piecewise-deterministic Markov process. Since in many applications the diffusion equation will be considered with periodic boundary conditions, we apply the theory of bilinear forms to prove existence and uniqueness of a solution, which is also shown to be positive, mass-preserving, and convergent to an equilibrium.

1 Introduction and motivation

In less generality and mathematical detail, the model we are going to discuss has been introduced in [8] in order to study the formation of keratin networks, which are a component of the cytoskeleton of biological cells. Due to the small diameter of keratin filaments of around $12nm$, microscopy techniques for visualizing single filaments are limited to electron microscopy, which does not allow for the observation of dynamical processes of network formation. Therefore, we developed a mathematical model simulating the formation of a keratin network and, in a recent study, were able to relate certain mechanisms of network growth to specific morphological properties of the network by computer simulation [8]. Although specifically designed for the application to keratin networks, the modeling approach is rather generic and lends itself readily to the modeling of other polymerization reactions in high spatiotemporal resolution. In the following we will motivate the model and discuss the mathematical framework, which is given by the concept of a piecewise-deterministic Markov process (PDMP). The key feature of this approach is that a feedback loop is established between a stochastic process determining locations, times and choices of macromolecular mechanisms of network growth events on the one hand and a deterministic evolution of a pool of soluble polymers fueling network growth on the other. The latter being modeled by the Laplace operator with periodic boundary conditions, we apply the theory of bilinear forms to prove existence and uniqueness of a solution to the initial value problem arising in the context of our model and prove that the solution is mass-preserving and positive. We will finally give a brief account on the application of the model to keratin network formation.

2 Model

Before the model is introduced in a mathematically precise way, we will outline and motivate its general concept. We consider network formation on a rectangular or cuboidal observation window $W = [0, \ell_1] \times \ldots \times [0, \ell_n]$, where for our applications the dimension n can be chosen as 2 or 3. Although protein networks in biological cells are generally 3D structures, the 2D case is also of practical interest, since in some cellular compartments the networks almost exhibit a 2D structure [6, 8] and 2D simulation results of the model can be directly related to 2D microscopy data. The state space is defined as $E = L^2(int(W)) \times \mathcal{S}(W)$, where the first component describes the concentration fields of soluble polymers fueling the network growth, and the second component $\mathcal{S}(W)$ is the space of all finite systems of line segments in W, which is used to model the filament network. By choosing an appropriate representation for a line segment by an initial point and the polar coordinates of its direction vector, $\mathcal{S}(W)$ can be considered as the state space of an object point process. Therefore, $\mathcal{S}(W)$ is a complete and separable metric space [18, 22] and $E = L^2(int(W)) \times \mathcal{S}(W)$ inherits these properties from its factors. Thus, our state space meets the topological requirements of Markov process theory. The choice to represent the network by a system of line segments was motivated by our specific biological application, where, given the spatial resolution, network formation proceeds by the addition of rather large elongated filament precursor molecules to the existing network structure. As a consequence, at this spatial scale of resolution network growth should not be considered as a time-continuous process. Instead, it is modeled by a random sequence $\tau_1, \tau_2 \ldots$ of network formation times, at which molecular building blocks transfer from the soluble pool of filament precursors into the filamentous phase. This is represented by the instantaneous addition of a further line segment to the segment system at the time of the growth event. The intensity of the process of network formation times varies in time, depending on the total amount of soluble polymers in the system and is thereby linked to the reaction kinetics of the system. Growth events can be of different type, e.g. a new filament can be initiated without contact to the existing network (nucleation) (Fig. 1(a)) or a new line segment can be appended to the end of an existing filament (elongation) (Fig. 1(b)). At each growth time τ_k, one of these or similar growth mechanism is chosen at random according to a probability distribution, which is controlled by model parameters and also depends on the current state of the system. Variation of these model parameters has been used in [8] in order to investigate the impact of single growth mechanisms on network architecture. Locations for the growth events in the observation window W are assigned randomly but the distribution reflects the current state of the concentration field of soluble polymers. More precisely, the probability of a location to be picked as a site for network growth depends on the locally available amount of soluble polymers. As soon as a network growth event takes place, the soluble pool is locally reduced by the amount of polymers consumed. Between these instantaneous local reductions of the soluble pool at the growth times τ_k, $k = 1, 2, \ldots$, the soluble polymers are regarded as permanently subjected to diffusion. Since in our application the number of soluble filament precursor molecules was relatively large, diffusion is not modeled by a set of random walks but by the classical diffusion equation

$$\frac{\partial c}{\partial t} = \kappa \triangle c$$

for some diffusion coefficient $\kappa > 0$, where $c(x, t)$ denotes the concentration of the soluble pool at location x and time t. Especially at higher concentration levels, this approach is computationally more efficient than modeling random walks of single molecules. Due to the fact that the model is designed to simulate network formation within a small compartment of the cytoplasm, which is not bounded by a membrane, periodic boundary conditions are

chosen, thus simulating the interaction of the observation window with a structurally similar environment.
From a more abstract point of view, the structure of the model outlined above combines a random sequence of jump times $\tau_1, \tau_2, \ldots$, at which the state is randomly and instantaneously changed, with a deterministic evolution during the time intervals (τ_k, τ_{k+1}), $k = 0, 2, \ldots$ (where we set $\tau_0 = 0$). This attributes the model to the class of piecewise-deterministic Markov processes, which has been introduced by Davis [9]. Although the concept can be further generalized [15, 21] we define a PDMP $\{X_t\}_{t\geq 0}$ mapping from some probability space into the state space E equipped with its Borel-σ algebra $\mathcal{B}(\mathcal{E})$ by the following four components:

1) an initial distribution α of X_0 on $(E, \mathcal{B}(E))$,

2) a C_0- semigroup
$$T : \mathbb{R}_+ \times E \longrightarrow E, \qquad (t, x) \mapsto T(t)x,$$
defining the evolution on the deterministic parts of the trajectories, more precisely, for all $t \in (\tau_k, \tau_{k+1})$ and given that $X_{\tau_k} = x$
$$X_t = T(t - \tau_k)x,$$

3) a transition function
$$Q : E \times \mathcal{B}(E) \longrightarrow [0, 1], \qquad (x, B) \mapsto Q(x, B),$$
where $Q(x, \cdot)$ is a probability measure for all $x \in E$ and $Q(\cdot, B)$ is measurable for all $B \in \mathcal{B}(E)$. Q governs the transition of X_t at the jump times τ_k by
$$\mathbb{P}(X_{\tau_k} \in B \mid \tau_k, X_{\tau_k -}) = Q(X_{\tau_k -}, B).$$

4) a jump intensity, which is a measurable function $\lambda : E \longrightarrow \mathbb{R}_+$ governing the conditional distribution of the jump times given the state of the system at the last jump by
$$\mathbb{P}(\tau_{k+1} - \tau_k \leq t \mid X_{\tau_k}) = 1 - \exp\left(-\int_0^t \lambda(T(v)X_{\tau_k})dv\right). \tag{2.1}$$

Note that by continuity of $T(\cdot)x$, the left limits $X_{\tau_k -} = \lim_{t\uparrow\tau_k} X_t$ are well-defined and the sample paths of a PDMP are right-continuous. The definition of the distribution of jump times given in (2.1) ensures that almost surely $0 < \tau_1 < \tau_2 < ...$, provided that $\tau_1, \tau_2, \ldots < \infty$, otherwise we set $\tau_k = \infty$ for all $k > k_0$. We will now specify these four components for our model.

2.1 Initial distribution

The initial network configuration can be modeled by any network model from stochastic geometry such as a random tessellation [7, 22]. For modeling the initial concentration field of soluble polymers a random field can be used. However, in order to obtain an admissible initial condition for the diffusion PDE, in view of the theory developed in section 3 the realizations of the random field must be in $L^2(intW)$ a.s. For applications it may also be desirable to work with an a.s. bounded random field. In case the model is applied to simulate the *de novo* formation of a network, the initial segment system is empty and it may also be plausible to consider a constant initial concentration field resembling the equilibrium of the soluble pool.

2.2 Jump intensity

By means of the state-dependent jump intensity λ the inter-occurrence times can be chosen as in the stochastic simulation algorithm for chemical reaction systems, which has been introduced by Gillespie [11], and thus, λ can be linked to global reaction kinetics. Following this approach λ, is chosen to be only dependent on the total amounts of the different species reacting. In our particular application the network formation process could be assumed to be dominated by the elongation of a roughly constant number of filament ends. As a consequence, the reaction kinetics was modeled to be of first order, which is reflected by defining

$$\lambda((c,s)) = K \int_{intW} c(x)dx$$

for any state $(c,s) \in L^2(intW) \times \mathcal{S}(W)$ and a reaction constant $K > 0$ [11, 12]. Since we will show later that the total number of soluble molecules is left unchanged by our particular choice of the semigroup T, the conditional distributions of the inter-occurrence times given the state $X_{\tau_k} = (X^{(1)}_{\tau_k}, X^{(2)}_{\tau_k})$ of the system after the last jump are of the form

$$\mathbb{P}(\tau_{k+1} - \tau_k \leq t \mid X_{\tau_k}) = 1 - \exp\left(-tK \int_{intW} X^{(1)}_{\tau_k}(x)dx\right).$$

The fact that λ is constant between jumps makes the model particularly favorable for computer simulation, since the inter-occurrence times simply have a conditionally exponential distribution. Even if in other applications the reaction kinetics should be of different order or dependent on the concentration of more than one species, this essential property of the model remains unchanged. In practical applications the network formation is considered to be finished once the total concentration drops under a certain threshold which does not allow for any more substantial polymerization.

2.3 Transition at the jump times

In view of Gillespie's stochastic simulation algorithm for reaction systems, our model can be regarded as an extension, which copies the time behaviour of Gillespie's algorithm but additionally monitors the reaction system in space. The spatial aspect of the network formation reaction is captured by the after jump distribution $Q(x,\cdot)$ of the PDMP, which is defined rather implicitly by a procedure determining a mechanism and a location of network growth according to a conditional probability distribution given the left limits of the (spatial) system configuration before the jump. The jump transitions additionally involve the choice of a possibly random length and orientation for the newly added network segment and consumption of soluble polymer pool.
In the following B_i, $i = 1, \ldots, \nu$, denotes the event that the network growth mechanism i is triggered. One could for example consider the case $\nu = 2$ and define B_1 as the addition of a new line segment on a location, which is not already occupied by a filament, and B_2 as the event that the new line segment is appended to a filament end. Thus, B_1 would correspond to a nucleation of a new filament and B_2 to filament elongation (Fig. 1), but in principle any other growth mechanism arising from a particular application can be incorporated into the model. At a jump time τ_k one of the mechanisms is picked according to the conditional probabilities

$$p_{i|(c,\xi)} = \mathbb{P}(B_i \mid X_{\tau_k -} = (c,\xi)),\ i = 1, \ldots, \nu,$$

given the left limit X_{τ_k-} of the state before the jump is (c,ξ), where $\sum_{i=1}^{\nu} p_{i|(c,\xi)} = 1$ for all $(c,\xi) \in E$. This way, we could for example model the elongation probabilities to be increasing in the number of possibly elongating filament ends or the nucleation probabilities to be dependent on the total amount of soluble polymers in the system. Once the mechanism of network growth has been determined, a location for the growth event is chosen. For this purpose the model exploits the information on the spatial distribution of the soluble polymer pool contained in the first component $X_t^{(1)}$ of the process. More precisely, the concentration field $X_{\tau_k-}^{(1)}$ immediately before the jump is used to construct a conditional probability distribution $\mathbb{P}(\cdot \mid B_i, X_{\tau_k-} = (c,\xi))$ on the Borel sets $\mathcal{B}(W)$ on the observation window such that locations with high local soluble polymer concentration are preferred sites of network growth. Notice that we are also conditioning on the network formation mechanism since the latter determines the set of potential growth locations. Elongation events for instance are naturally restricted to the set of filament ends $s(\xi)$ and we could e.g. define

$$\mathbb{P}(\cdot \mid B_2, X_{\tau_k-} = (c,\xi)) = \sum_{z \in s(\xi) \cap A} \frac{\int_{b(z,\rho)} c(x)dx}{\sum_{y \in s(\xi)} \int_{b(y,\rho)} c(x)dx}, \tag{2.2}$$

where $b(y,\rho)$ denotes the ball of radius ρ centered at y. Following the concept of periodic boundaries applied for the diffusion process of the soluble polymers, parts of these balls protruding W are understood to be shifted to the opposite side. By the transformation of the deterministically evolving concentration field into a spatial probability distribution the model interprets the solutions of the diffusion PDE stochastically. This way it is reflected that the diffusion PDE can be viewed as a mean value approach to random walks of single molecules by its relation to Brownian motion (cf. [16]).
The direction of the line segment added to the network is determined by some probability distribution on the unit sphere, which may also be conditional on the state of the system, the growth mechanism and the growth location, since e.g. elongation events may need to respect physical curvature restrictions of the filaments.
Depending on the application, the length of the randomly added line segment can either be modeled as deterministic or as realization of a random variable.
We will now specify the feedback of growth events on the concentration field of soluble polymers. Before soluble polymers are consumed, a new line segment S_{τ_k} has been determined as described above. The dilation $S_{\tau_k} \oplus b(o,r)$ of S_{τ_k} denotes all points in the observation window whose distance to S_{τ_k} is no more than r, where parts of the segment dilations protruding the observation window are shifted to the opposite side. We will show in Section 3 that the solution of the diffusion PDE yields space-continuous concentration fields $c(t,x)$ for any initial condition in $c(0,x) \in L^2(intW)$ once $t > 0$. As a consequence, if $0 < \tau_1 < \tau_2 < \ldots$, then there is a well defined dilation $S_{\tau_k} \oplus b(0,r)$ containing exactly the number γ of molecules consumed for network growth, i.e.

$$\int_{S_{\tau_k} \oplus b(0,r)} c(x)dx = \gamma.$$

Notice however, that this dilation only exists if the total number of soluble molecules is high enough, which does not pose a problem in applications, since concentration levels of soluble polymers would be so low that they would not allow for substantially more polymerization.
We define the concentration field immediately after network formation by

$$X_{\tau_k}^{(1)}(x) = \begin{cases} 0 & \text{if } x \in S_{\tau_k} \oplus b(0,r), \\ X_{\tau_k-}^{(1)}(x) & \text{else.} \end{cases}$$

Note that this concentration field serves as the initial condition for soluble pool diffusion after time τ_k.

2.4 The semigroup

During the time intervals (τ_k, τ_{k+1}), $k = 0, 1, \ldots$ the network configuration is constant, whereas the soluble pool is subjected to diffusion. In many applications the reaction is observed on a window which is not physically bounded (e.g. by a membrane) and it can be assumed that the diffusion process interacts with a structurally similar environment. This situation is reflected by considering periodic boundary conditions for the diffusion PDE. In the next section we will construct the Laplace operator with periodic boundary conditions and see that it generates a semigroup $T(t)$ on $L^2(intW)$, which yields the unique solution to the diffusion PDE for any of the bounded initial conditions arising in the context of our model. The semigroup acting on both factors of the state space of our PDMP is then given by

$$\widetilde{T}(t)(c, \xi) = (T(t)c, \xi), \quad \text{for all } (c, \xi) \in E.$$

3 The Laplace operator with periodic boundary conditions

Since in stochastic geometry W usually denotes a closed observation window and the Laplace operator we are going to construct is defined on a subspace of the L^2 functions on some open domain, for ease of notation, we will not denote this domain by $intW$ but by Ω. In the following, Ω will be of the form $\Omega = (0, \ell_1) \times \ldots \times (0, \ell_n)$ and we will construct the Laplace operator with periodic boundaries as the associated operator of a bilinear form on some appropriately chosen function space $V \subset L^2(\Omega)$, which is defined via the trace operator. We will see that the Laplace operator on V generates a C_0-semigroup on $L^2(\Omega)$, which serves to obtain a solution $c(t, x)$ of the initial value problem

$$\frac{\partial c}{\partial t} = \kappa \triangle c, \quad \text{for } t > 0 \quad \text{and} \quad c(0, x) = f(x), \tag{3.3}$$

where $c(t, x)$ is in V for all $t > 0$ and, as a consequence, $c(t, x)$ has a periodic boundary for all $t > 0$. The constant $\kappa > 0$ is the diffusion coefficient. We will prove that the solution is positive once $f > 0$ and preserves the total number of particles in the system.

As mentioned above, the construction of V is based on the following trace theorem [1].

Theorem 3.1 *Let $\Omega \subset \mathbb{R}^n$ be open and bounded with Lipschitz-boundary. Then there exists a unique continuous linear operator $\mathbf{S} : H^1(\Omega) \longrightarrow L^2(\partial\Omega)$, such that*

$$\mathbf{S}u = u|_{\partial(\Omega)} \quad \textit{for } u \in H^1(\Omega) \cap C^0(\overline{\Omega}).$$

By convention, the set $H^1(\Omega) \cap C^0(\overline{\Omega})$ denotes the collection of all functions in the first Sobolev space $H^1(\Omega) := \{u \in L^2(\Omega) : D_j u \in L^2(\Omega), j = 1, \ldots, n\}$ which are continuous up to the boundary. The image of such a function under the trace operator is obtained by considering its continuous extension to the closure of Ω and then taking the restriction of this extension to the boundary. An open and bounded subset $\Omega \subset \mathbb{R}^n$ has a Lipschitz boundary,

if $\partial\Omega$ can be covered by finitely many open sets $U_1, \ldots, U_m$ such that $\partial\Omega \cap U_j$, $j = 1, \ldots, m$, is the graph of a Lipschitz continuous function and each set $\Omega \cap U_j$ lies on one side of this graph (for a mathematically precise definition see [1]). In particular, every cuboid in $\mathbb{R}^n$ has a Lipschitz boundary. Therefore, for our particular case $\Omega = (0, \ell_1) \times \ldots \times (0, \ell_n)$ we may define the function space $V \subset H^1(\Omega)$ as

$$V = \{u \in H^1(\Omega) : \mathbf{S}u((x_1, \ldots, x_{i-1}, 0, x_{i+1}, \ldots, x_n)) = \mathbf{S}u((x_1, \ldots, x_{i-1}, \ell_i, x_{i+1}, \ldots, x_n)),$$
$$\text{where } (x_1, \ldots, x_{i-1}, x_{i+1}, \ldots, x_n) \in (0, \ell_1) \times \ldots \times (0, \ell_{i-1}) \times (0, \ell_{i+1}) \times \ldots \times (0, \ell_n),$$
$$i = 1, \ldots, n\}.$$

Proposition 3.1 *The function space V is a Hilbert space. Moreover, $V \overset{d}{\hookrightarrow} L^2(\Omega)$, i.e., V is continuously and densely injected in $L^2(\Omega)$.*

Proof.

(i) $\mathbf{S}$ is continuous and V is the pre-image of the elements in $L^2(\partial\Omega)$ having a periodic boundary, which form a closed set in $L^2(\partial\Omega)$. Thus, V is closed in the Hilbert space $H^1(\Omega)$ and, consequently, a Hilbert space itself with the inner product

$$(u, v)_V = (u, v)_{H^1} = (u, v)_{L^2} + \int_\Omega \nabla v \nabla u dx,$$

where gradients are defined in the weak sense.

(ii) The space of test functions $C_c^\infty(\Omega)$ is dense in $L^2(\Omega)$ [23]. Moreover, $C_c^\infty(\Omega) \subset V$ by the properties of $\mathbf{S}$. Consequently, V is dense in $L^2(\Omega)$.

(iii) The injection is continuous since

$$\|f\|_V^2 = \|f\|_{H^1}^2 = \|f\|_{L^2}^2 + \int_\Omega \nabla f \nabla f dx \geq \|f\|_{L^2}^2.$$

□

As we will see below, the Laplace operator on V can be obtained as the associated operator of the bilinear form $a : V \times V \to \mathbb{R}$ defined as

$$a(u, v) = \kappa \int_\Omega \nabla u \nabla v dx,$$

where we consider weak gradients.

Proposition 3.2 *The bilinear form $a(\cdot, \cdot)$ is continuous and $L^2(\Omega)$-elliptic, i.e., there exist $w \in \mathbb{R}$ and $\alpha > 0$ such that $a(u, u) + w\|u\|_{L^2}^2 \geq \alpha\|u\|_V^2$ for all $u \in V$.*

Proof.

1. Continuity follows by the Cauchy-Schwarz inequality, since

$$|a(u, v)| = |\kappa \textstyle\int_\Omega \nabla u \nabla v dx| = \kappa| \textstyle\int_\Omega uv dx + \int_\Omega \nabla u \nabla v dx - \int_\Omega uv dx|$$

$$\leq \kappa|(u, v)_V| + \kappa|(u, v)_{L^2}| \leq \kappa\|u\|_V\|v\|_V + \kappa\|u\|_{L^2}\|v\|_{L^2} \leq 2\kappa\|u\|_V\|v\|_V.$$

2. By Proposition 3.1 $V \overset{d}{\hookrightarrow} L^2(\Omega)$, thus for proving ellipticity it suffices to note that

$$a(u,u) + \kappa\|u\|_{L^2}^2 = \kappa \int_\Omega \nabla u \nabla u dx + \kappa \int_\Omega u^2 dx = \kappa\|u\|_V^2.$$

□

As a consequence of being elliptic and continuous $a(\cdot,\cdot)$ has a densely defined associated operator A_a with domain $D(A_a)$ [20], where

$$D(A_a) = \{u \in V : a(u,v) = (f,v)_{L^2(\Omega)} \text{ for some } f \in L^2(\Omega) \text{ and for all } v \in V\},$$
$$A_a(u) = f.$$

For $u \in L^2(\Omega)$ we define $\triangle u \in L^2(\Omega)$ if there exists $g \in L^2(\Omega)$ such that

$$\int_\Omega u \triangle \varphi dx = \int_\Omega g\varphi dx \text{ for all} \varphi \in C_c^\infty(\Omega).$$

In that case g is unique and we write $\triangle u := g$ (the weak Laplacian of u).
Our next observation is that $-A_a$ is a realization of $\kappa\triangle$ with periodic boundary conditions.

Proposition 3.3 *The operator A_a is selfadjoint and given by*

$$A_a u = -\kappa \triangle u \text{ for } u \in D(A_a) \subset \{u \in V : \triangle u \in L^2(\Omega)\}$$

.

Proof. Since the form $a(\cdot,\cdot)$ is symmetric, the associated operator A_a is selfadjoint. Let $u \in D(A_a)$, $A_a u = f$. Then $u \in V$ and in particular $u \in H^1(\Omega)$. Hence, for all $\varphi \in C_c^\infty(\Omega)$ one has

$$< -\kappa\triangle u, \varphi >= -\kappa \int_\Omega u \triangle \varphi dx = \kappa \int_\Omega \nabla u \nabla \varphi dx = a(u,\varphi) = \int_\Omega f\varphi dx.$$

This shows that $-\kappa\triangle u = f$ in the sense of distributions and we have shown that $D(A_a) \subset \{u \in V : \triangle u \in L^2(\Omega)\}$.

□

The semigroup $\{T(t)\}_{t\geq 0}$ generated by $-A_a$ governs the parabolic initial value problem on Ω. The properties of the solution are described in the following result (cf. [2], Theorem 1.1).

Theorem 3.2 *Let $f \in L^2(\Omega)$ be given. Then $T(t)f \in C^\infty(\Omega)$ and letting $c(t,x) = (T(t)f)(x)$ we obtain the unique solution of*

$$\begin{cases} c \in C^\infty(0,\infty) \times \Omega, \\ \frac{\partial}{\partial t} c = \kappa \triangle c \text{ on } (0,\infty) \times \Omega, \\ \lim_{t\downarrow 0} c(t,\cdot) = f \text{ in } L^2(\Omega), \\ c(t,\cdot) \in V. \end{cases}$$

Now it follows from [2], Theorem 1.5, that the semigroup is *strictly positive*, i.e.,

$$(T(t)f)(x) > 0 \text{ for all } x \in \Omega, t > 0$$

whenever $f \in L^2(\Omega)$ such that $f \geq 0$ a.e. and f does not vanish almost everywhere.
From [3](3.5.1) it can be deduced that the semigroup converges to an equilibrium. More precisely, let

$$Pf = \frac{1}{|\Omega|} \int_\Omega f(x)dx \mathbb{1}_\Omega.$$

Then P is an orthogonal projection of rank 1.

Proposition 3.4 *One has* $\lim_{t\to\infty} T(t) = P$ *in* $\mathcal{L}(L^2(\Omega))$.

Proof. Since the injection $H^1(\Omega) \hookrightarrow L^2(\Omega)$ is compact by Rellich's Theorem, and the semigroup T is holomorphic, it follows that $T(t)$ is compact for $t > 0$. Since $a(u, u) \geq 0$ for all $u \in V$ it follows that $\|T(t)\|_{\mathcal{L}(L^2(\Omega))} \leq 1$. Thus the spectrum of $-A_a$ is included in $(-\infty, 0]$.
Let $e_1 = \frac{1}{|\Omega|}\mathbb{1}_\Omega$. Then $e_1 \in D(A_a)$ and $A_a e_1 = 0$. Since the semigroup is strictly positive it follows from the Krein-Rutman Theorem that the first eigenvalue 0 of A_a is simple. Now the claim follows from the spectral theorem.

□

From Proposition 3.4 we deduce that the solution is mass-preserving, i.e., it preserves the number of particles in the system.

Proposition 3.5 *Let* $f \in L^2(\Omega)$. *Then*

$$\int_\Omega T(t)f dx = \int_\Omega f dx \qquad \text{for all } t \geq 0.$$

Proof. Since $T(t)P = \lim_{s\to\infty} T(s)T(t) = \lim_{s\to\infty} T(t + s) = P$, one has $T(t)P = P$ for all $t \geq 0$. By using that $T(t)$ is selfadjoint it follows that

$$\textstyle\int_\Omega T(t)f dx = (T(t)f, P\mathbb{1}_\Omega)_{L^2} = (f, T(t)P\mathbb{1}_\Omega)_{L^2} = (f, P\mathbb{1}_\Omega)_{L^2} = \int_\Omega f dx.$$

□

4 Aspects of an application to the modeling of keratin networks

In order to illustrate the relevance of the model for applications we will briefly summarize, how it was used to investigate the formation process of a keratin network in [8]. The description given here will only emphasize structural aspects of the model and provide an idea of the type of questions that may be investigated by means of this modeling approach. For more details we refer to [8].
Due to specific biochemical properties of the keratin polymers forming the filaments of the network, network architecture defines the viscoelastic properties of the cell at large deformations [5]. It has been demonstrated that even small alterations of network architecture can significantly change the elasticity of polymer networks networks in biological cells and,

hence, the mechanical properties of cellular compartments and the entire cell [10]. Changes in network morphology such as investigated in [6, 7] have therefore been linked to regulation of cell motility and migration [4]. Mathematical modeling of network assembly processes can thus contribute to a better understanding of these phenomena. For the formation of keratin networks the very thin peripheral compartments of a cell are particularly relevant [24]. In these areas keratin networks exhibit an almost planar structure [6, 7] and therefore we considered a 2D observation window. The set of network formation mechanisms incorporated into the model was motivated by particular biochemical properties of keratin oligomers and experimental data [13, 24]. All growth mechanisms were represented by the addition of a line segment of deterministic length to the network. The segment length was chosen as the size of a so-called unit-length filament (ULF). ULFs are the basic macromolecular building blocks of keratin filaments [17]. As a first mechanism we considered filament nucleation (Fig. 1(a)), which, in terms of the model, is the addition of a line segment whose location is selected independently of the current network configuration. In contrast, new filaments could also be initiated by lateral annealing of keratin oligomers at a preexisting filament, thus forming a Y-junction in the network graph (Fig. 1(c)). Once a filament had been initiated either by means of nucleation or lateral annealing it started an elongation process, i.e. new line segments were possibly appended to the free filament ends (Fig. 1(b)). For the definitions of the probability distributions governing the choice of growth locations in dependency of the concentration fields of soluble oligomers we refer to [8]. The definition for the case of an elongation event is given in (2.2).

Specifically for the 2D case, the model behavior at the times of network growth was extended by the mechanism of filament merging. This means that once a filament intersected the preexisting network as the result of a growth event, the model decided at random whether the filaments entangled and a network node of degree 3 was formed (Fig. 1(d)) or the filaments were only crossing each other yielding a node of degree 4 (Fig. 1(e)). The merging probability was a fixed model parameter, which could be used to control the distribution of node degrees. Since on electron microscopy images keratin filaments exhibit only marginal curvature, we only considered straight filament elongations [6, 7]. Directions of newly initiated filaments by nucleation or lateral annealing were modeled as uniformly distributed on the unit sphere, since there are no statistically significant indications of preferred filament orientations on electron microscopy data [6]).

By variation of the rates at which the different growth mechanisms were triggered, these could be related to morphological properties of the networks, the latter being quantified by tools from spatial statistics and graph theory. One of the most interesting findings was that the mechanism of lateral annealing accounted for the formation of mesh clusters (Fig. 2), which can also be found on microscopy data of keratin networks. Thus, regulation of lateral annealing events may enable the cell to modify local as well as global mechanical properties by changing the network configuration from a spatially homogeneous to a clustered state at constant total network length. Finite element modeling as applied in [14] may be used to link network morphology and cell mechanics and scrutinize this hypothesis.

Even if transport of molecules within the cytoplasm is in general a process of substantially higher complexity than simple diffusion, modeling of the soluble filament precursor molecules by the diffusion PDE allowed us to study network formation in dependency of the spatiotemporal distribution of the soluble filament precursor molecules. Monitoring of the concentration fields could be used to check whether zones of soluble pool depletion occurred, which indicated diffusion limitations of the network formation scenario under consideration (Fig. 3). Scenarios leading to mesh clustering for instance, resulted in high local consumption of soluble polymers around the emerging clusters. As a consequence, mesh clustering was even

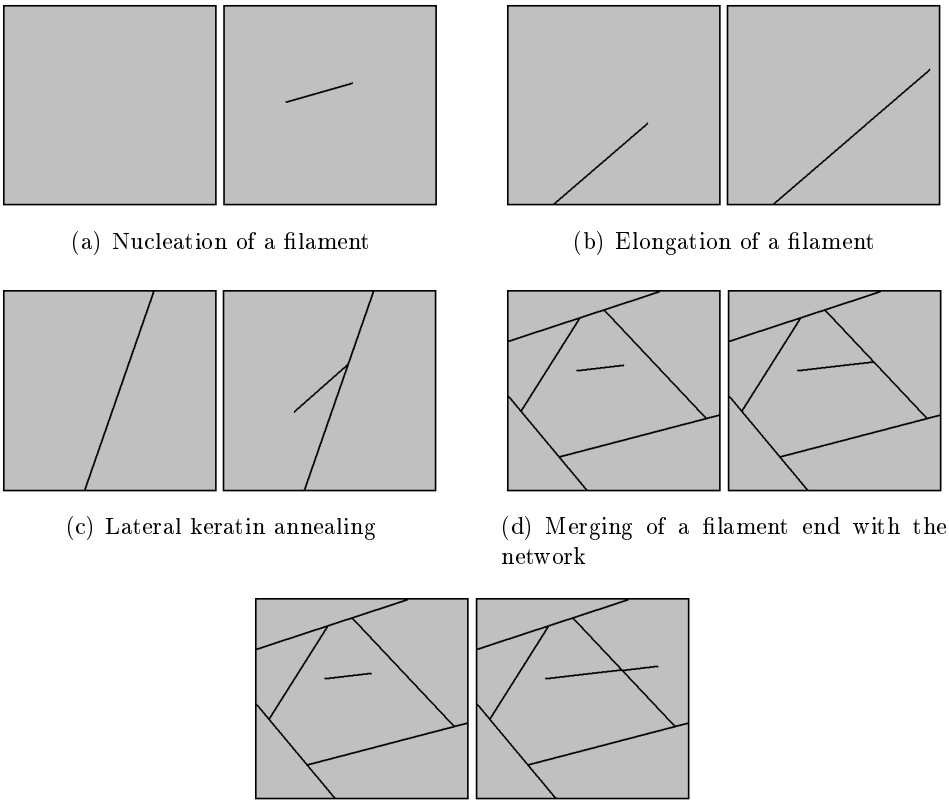

(a) Nucleation of a filament

(b) Elongation of a filament

(c) Lateral keratin annealing

(d) Merging of a filament end with the network

(e) Crossing of two filaments

Figure 1: Mechanisms of network formation

suppressed if the diffusion coefficient was not chosen high enough to rapidly compensate for the local loss of soluble pool triggered by filament growth. Nevertheless, under realistic diffusion coefficients [19] the reaction system was not diffusion limited for all scenarios of network growth we considered.

5 Concluding remarks

Using the modeling approach of a PDMP, we were able to add a spatial resolution to the established stochastic simulation algorithm for chemical reactions by integrating elements from stochastic geometry and the deterministic diffusion PDE with periodic boundary conditions. This yielded a mathematically consistent model, which is particularly appropriate for computer simulation and may be adapted easily to a variety of other applications than keratin network formation. Diffusion equations with periodic boundary conditions naturally arise in the modeling of spatiotemporal reaction systems, whenever the observation window is surrounded by a structurally similar environment but not bounded. The theory of bilinear forms lends itself readily to the mathematical investigation of the diffusion PDE with these boundary conditions by considering an appropriate function space. The diffusion PDE does not reflect transport processes in biological cells in their entire complexity. Nevertheless, once the reacting species are present in a certain abundance, integration of the PDE into the model allows to elucidate principle spatiotemporal aspects of a reaction in a computationally

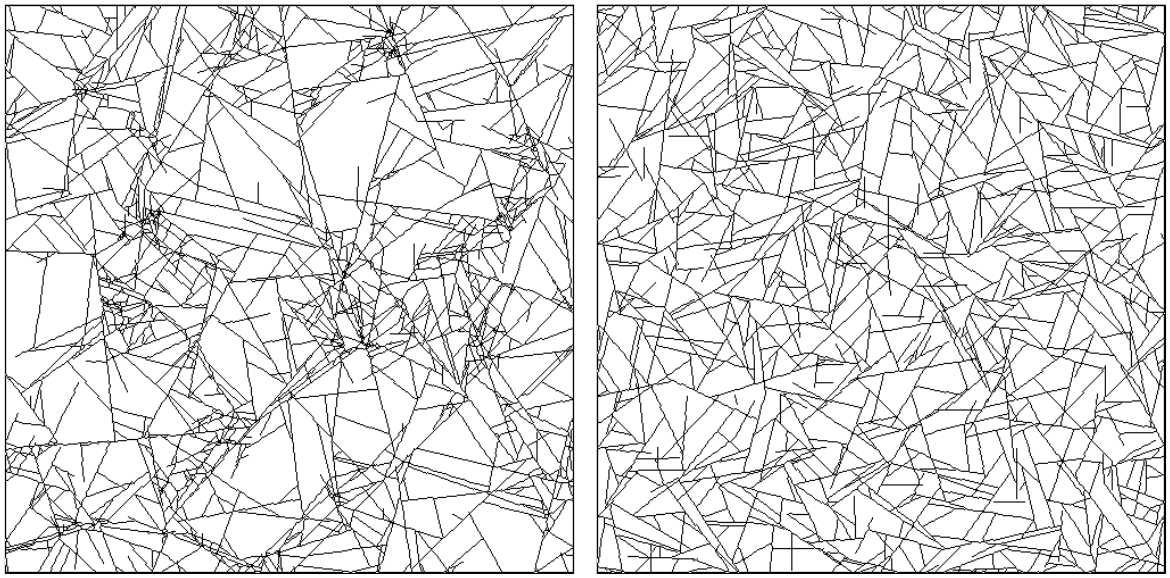

(a) (b)

Figure 2: Response of network morphology to the frequency of lateral annealing events. A high rate of lateral annealing events caused the formation of mesh clusters (a), whereas simulations without lateral annealing events yielded spatially homogeneous networks (b).

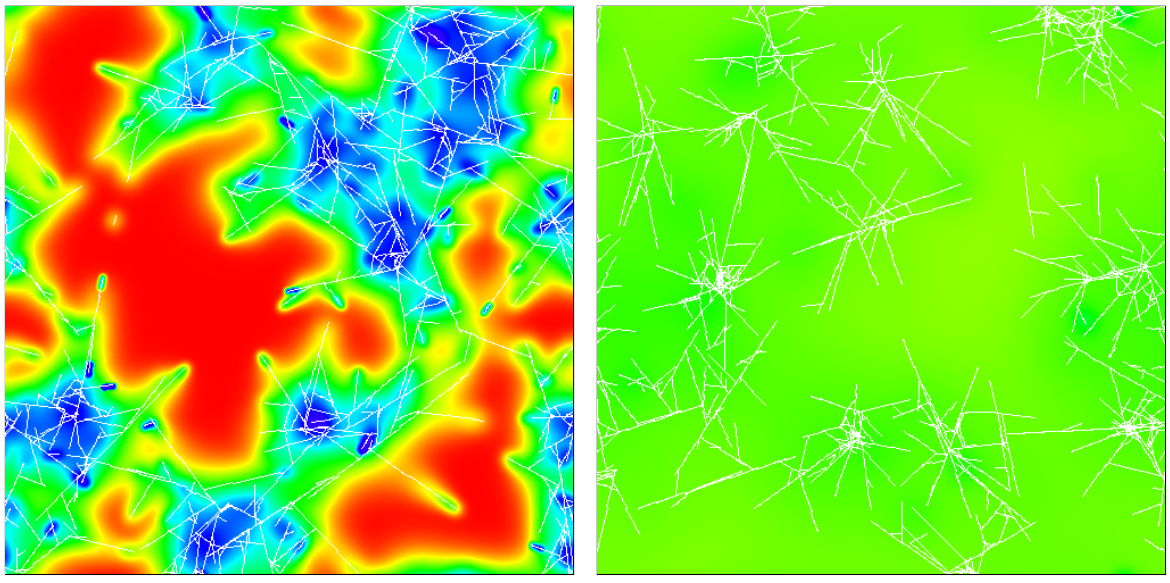

(a) (b)

Figure 3: Concentration fields of soluble filament precursor molecules during network formation. Very small diffusion coefficients resulted in depletion zones (blue areas) (a), whereas at higher diffusion coefficients (b) the soluble pool was evenly spread over the observation window.

efficient way. Combining a PDE with stochastic modeling of rare events, PDMPs are a flexible class of models capturing spatial and temporal aspects of biochemical reaction systems in high resolution.

Acknowledgements. This work was supported by grants from Deutsche Forschungsgemeinschaft to MB and VS (SFB 518 projects B21 and B22). SP was supported by NSERC Discovery Grant.

References

[1] H.W. Alt (2006) *Lineare Funktionalanalysis.* Springer, Berlin

[2] W. Arendt (2001) Different domains induce different heat semigroups on $C_0(\Omega)$. *Evolution Equations and Their Application in Physics and Life Sciences* G. Lumer, L. Weis eds. , Marcel Dekker, New York 1–14.

[3] W. Arendt (2004) Semigroups and evolution equations: functional calculus, regularity amd kernel estimates. *Handbook of Differential Equations, Evolutionary Equations, 1* C.M. Dafermos and E. Feireisl eds., Elsevier 1–85.

[4] C. Ballestrem, B. Wehrle-Haller, B. Hinz, B.A. Imhof (2000) Actin-dependent lamellipodia formation and microtubule-dependent tail retraction control directed cell migration. Mol. Biol. Cell 11, 2999–3012.

[5] M. Beil, A. Micoulet, G. von Wichert, S. Paschke, P. Walther, M.B. Omary, P.P. Van Veldhoven, U. Gern, E. Wolff-Hieber, J. Eggermann, J. Waltenberger, G. Adler, J. Spatz, T. Seufferlein (2003) Sphingosylphosphorycholine regulates keratin network architecture and visco-elastic properties of human cancer cells. Nat. Cell Biol. 5, 803–811.

[6] M. Beil, H. Braxmeier, F. Fleischer, V. Schmidt, P. Walther (2005) Quantitative analysis of keratin filament networks in scanning electron microsopy images of cancer cells. J. Microsc. 220, 84–95.

[7] M. Beil, S. Eckel, F. Fleischer, H. Schmidt, V. Schmidt, P. Walther (2006) Fitting of random tessellation models to keratin filament networks. J. Theor. Biol. 241(1), 62–72.

[8] M. Beil, S. Lück, F. Fleischer, S. Portet, W. Arendt, V. Schmidt (2008) Simulating the formation of keratin filament networks by a piecewise-deterministic Markov process. J. Theor. Biol., doi:10.1016/j.jtbi.2008.09.044

[9] M.H.A. Davis (1984) Piecewise-deterministic Markov processes: a general class of non-diffusion stochastic models. J. Roy. Stat. Soc. B 46(3), 353–388.

[10] F. Fleischer, R. Ananthakrishnan, S. Eckel, H. Schmidt, J. Käs, T. Svitkina, V. Schmidt, M. Beil (2007) Actin network architecture and elasticity in lamellipodia of melanoma cells. New J. Phys. 9, 420.

[11] D.T. Gillespie (1977) Exact stochastic simulation of coupled chemical reactions. J. Phys. Chem. 81(25), 2340–2361.

[12] D.T. Gillespie (1992) A rigorous derivation of the chemical master equation. Physica A 188, 404–425.

[13] H. Herrmann, U. Aebi (2000) Intermediate filaments and their associates: multi-talented structural elements specifying cytoarchitecture and cytodynamics. Curr. Opin. Cell Biol. 12, 79–90.

[14] C. Heussinger, E. Frey (2006) Stiff polymers, foams, and fiber networks. Phys. Rev. Lett. 96, 017802.

[15] M. Jacobsen (2006) *Point Process Theory and Applications.* Birkhäuser, Boston.

[16] I. Karatzas, S.E. Shreve (1998) *Brownian Motion and Stochastic Calculus* Springer, New York.

[17] R. Kirmse, S. Portet, N. Mucke, U. Aebi, H. Herrmann, J. Langowski (2007) A quantitative kinetic model for the in vitro assembly of intermediate filaments from tetrameric vimentin. J. Biol. Chem. 282, 18563–18572.

[18] K. Matthes, J. Kerstan, J. Mecke (1976) *Infinitely Divisible Point Processes.*J. Wiley & Sons, New York.

[19] S. Portet, O. Arino, J. Vassy, D. Schoevaert (2003) Organization of the cytokeratin network in an epithelial cell. J. Theor. Biol. 223, 313–333.

[20] E. Ouhabaz (2005) *Analysis of Heat Equations on Domains.* Princeton University Press, Oxford.

[21] T. Rolski, H. Schmidli, V. Schmidt, J. Teugels (1999) *Stochastic Processes for Insurance and Finance.* J. Wiley and Sons, Chichester.

[22] R. Schneider, W. Weil (2008) *Stochastic and Integral Geometry.* Springer, Berlin.

[23] D. Werner (2005) *Funktionalanalysis.* Springer, Berlin.

[24] R. Windoffer, S. Woll, P. Strnad, R.E. Leube (2004) Identification of novel principles of keratin filament network turnover in living cells. Mol. Biol. Cell 15, 2436–2448.

Sebastian Lück and Volker Schmidt, Institute of Stochastics, Ulm University, D-89069 Ulm, Germany
E-mail addresses: sebastian.lueck@uni-ulm.de, volker.schmidt@uni-ulm.de

Michael Beil, Department of Internal Medicine I, University Hospital Ulm, D-89070 Ulm, Germany
E-mail address: michael.beil@uni-ulm.de

Frank Fleischer, Medical Data Services/Biostatistics, Boehringer Ingelheim Pharma GmbH & Co. KG, D-88397 Biberach, Germany
E-mail address: frank.fleischer@boehringer-ingelheim.com

Stéphanie Portet, Department of Mathematics, University of Manitoba, Winnipeg, Manitoba, Canada, R3T 2N2
E-mail address: portets@cc.umanitoba.ca

Wolfgang Arendt, Institute of Applied Analysis, Ulm University, D-89069 Ulm, Germany
E-mail address: wolfgang.arendt@uni-ulm.de